frontiers in Physiology

ORIGINAL RESEARCH
published: xx August 2018
doi: 10.3389/fphys.2018.01186

Calcitriol, the Bioactive Metabolite of Vitamin D, Increases Ventricular K^+ Currents in Isolated Mouse Cardiomyocytes

María Tamayo[1], Laura Martin-Nunes[1], Almudena Val-Blasco[2], Maria J. Piedras[1,3], María J. Larriba[4], Nieves Gómez-Hurtado[1], María Fernández-Velasco[2] and Carmen Delgado[1]**

[1] Biomedical Research Institute "Alberto Sols" CSIC-UAM/CIBER-CV, Madrid, Spain, [2] Innate Immune Response Group, IdiPAZ/CIBER-CV, La Paz University Hospital, Madrid, Spain, [3] University Francisco de Vitoria, Madrid, Spain, [4] Biomedical Research Institute "Alberto Sols" CSIC-UAM/CIBERONC, Madrid, Spain

Calcitriol, the bioactive metabolite of vitamin D, interacts with the ubiquitously expressed nuclear vitamin D receptor (VDR) to induce genomic effects, but it can also elicit rapid responses via membrane-associated VDR through mechanisms that are poorly understood. The down-regulation of K^+ currents is the main origin of electrophysiological remodeling in pathological hypertrophy and heart failure (HF), which can contribute to action potential prolongation and subsequently increase the risk of triggered arrhythmias. Adult mouse ventricular myocytes were isolated and treated with 10 nM calcitriol or vehicle for 15–30 min. In some experiments, cardiomyocytes were pretreated with the Akt inhibitor triciribine. In the adult mouse ventricle, outward K^+ currents involved in cardiac repolarization are comprised of three components: the fast transient outward current (I_{tof}), the ultrarapid delayed rectifier K^+ current (I_{kur}), and the non-inactivating steady-state outward current (I_{ss}). K^+ currents were investigated using the whole-cell or the perforated patch-clamp technique and normalized to cell capacitance to obtain current densities. Calcitriol treatment of cardiomyocytes induced an increase in the density of I_{tof} and I_{kur}, which was lost in myocytes isolated from VDR-knockout mice. In addition, calcitriol activated Akt in cardiomyocytes and pretreatment with triciribine prevented the calcitriol-induced increase of outward K^+ currents. In conclusion, we demonstrate that calcitriol via VDR and Akt increases both I_{tof} and I_{kur} densities in mouse ventricular cardiomyocytes. Our findings may provide new mechanistics clues for the cardioprotective role of this hormone in the heart.

Keywords: calcitriol, potassium currents, cardiomyocytes, vitamin D, cellular electrophysiology, ionic channel remodeling, Akt

OPEN ACCESS

Edited by:
T. Alexander Quinn, Dalhousie University, Canada

Reviewed by:
Robert Alan Rose, University of Calgary, Canada
Fátima Regina Mena Barreto Silva, Universidade Federal de Santa Catarina, Brazil

****Correspondence:***
María Fernández-Velasco
maria.fernandez@idipaz.es
Carmen Delgado
cdelgado@iib.uam.es

Specialty section:
This article was submitted to Cardiac Electrophysiology, a section of the journal Frontiers in Physiology

Received: *14 May 2018*
Accepted: *07 August 2018*
Published: *xx August 2018*

Citation:
Tamayo M, Martin-Nunes L, Val-Blasco A, Piedras MJ, Larriba MJ, Gómez-Hurtado N, Fernández-Velasco M and Delgado C (2018) Calcitriol, the Bioactive Metabolite of Vitamin D, Increases Ventricular K^+ Currents in Isolated Mouse Cardiomyocytes. Front. Physiol. 9:1186. doi: 10.3389/fphys.2018.01186

INTRODUCTION

Cardiac remodeling is the response of the heart to various damaging stimuli, such as long standing hypertension or myocardial infarction. This physiological process is characterized by the triggering of "compensatory" pathways such as, the renin-angiotensin system (RAS) and the sympathetic nervous system (SNS). Initially, this mechanism is beneficial but sustained activation

of neurohormonal systems can cause additional damage to the heart, commonly in the form of hypertrophy, apoptosis and fibrosis, contributing to the adverse remodeling process, and accelerating the transition toward heart failure (HF) (Heusch et al., 2014; Hartupee and Mann, 2017). Moreover, ventricular remodeling modifies the functioning of ion channels and transporters such as that cardiac rhythm disturbances occur, which is termed "arrhythmogenic remodeling" (Nattel et al., 2007). K^+ currents play key roles in shaping the action potentials (APs), and adverse ventricular remodeling induces down-regulation of several K^+ currents, which are associated with prolonged QT intervals, increased risk of malignant arrhythmias and sudden cardiac death. It is well known that almost one-half of HF patients die from sudden cardiac death, most probably due to ventricular arrhythmias (Nass et al., 2008; Lehnart et al., 2009).

Vitamin D deficiency is highly prevalent worldwide, an in particular among the elderly population (Holick, 2007). Low levels of vitamin D have been associated with worse outcomes in patients with HF (Liu et al., 2011; Gotsman et al., 2012) and vitamin D supplementation has been shown to ameliorate symptoms and decrease mortality (Gotsman et al., 2012; Witte et al., 2016). The biologically active form of vitamin D is 1,25-dihydroxycholecalciferol or calcitriol, which translocates the cell membrane and cytoplasm to reached the nucleus of the cell, where it binds to vitamin D receptor (VDR). In turn, VDR can bind to retinoic X receptor to serve as a nuclear transcription factors, regulating the expression of numerous genes. In addition to these genomic responses, calcitriol can mediate rapid responses by binding to cell membrane VDR, interacting with ion channels (Menegaz et al., 2011; Zanatta et al., 2012; Tamayo et al., 2017) and membrane-based signaling pathways (Larriba et al., 2014).

Previous reports have postulated that activation of the PI3K pathway can modulate cardiac K^+ channels in cardiomyocytes (Yang et al., 2012; Gomez-Hurtado et al., 2014) and Akt is a well-known target of PI3K, activated by calcitriol in other cellular systems.

Calcitriol has been demonstrated to initiate a VDR-dependent rapid activation of PI3K/Akt signaling in osteoblasts (Vertino et al., 2005). In addition, the anti-apoptotic properties of calcitriol in osteoblasts are thought to be related to the non-genomic activation of a VDR/PI3K/Akt pathway (Zhang and Zanello, 2008). Moreover, activation of Akt by calcitriol has also been observed in leukemia, squamous cell carcinoma and skeletal muscle cells (Ma et al., 2006; Zhang et al., 2006; Buitrago et al., 2012).

Vitamin D receptor has been identified in numerous cardiovascular cell types including cardiomyocytes (Tishkoff et al., 2008; Norman and Powell, 2014). Whereas experimental studies have demonstrated rapid effects of calcitriol on cardiac calcium channels (Zanatta et al., 2012; Tamayo et al., 2017), its effects on cardiac potassium channels remain elusive. Thus, in the present study we used patch-clamp recordings to examine the rapid responses of calcitriol on the main K^+ currents responsible for cardiac repolarization in the mouse and the potential mechanism (s) involved. Our results show that calcitriol increases outward K^+ current densities in ventricular myocytes via Akt signaling, and that this mechanism can contribute to the protective effect of vitamin D on the heart.

MATERIALS AND METHODS

Animals

Adult (2–3 months old) male C57BL/6J mice and VDR knockout (KO) mice were originally generated by Dr. Marie Demay (Harvard Medical School, Boston, MA, United States) (Li et al., 1997) and kindly donated by Dr Alberto Muñoz (Biomedical Research Institute "Alberto Sols" CSIC-UAM, Madrid, Spain) were used. All experiments on mice were performed after approval by the Bioethical Committee of the *Consejo Superior de Investigaciones Cientificas* following recommendations of the Spanish Animal Care and Use Committee (Proex 035-15) according to the guidelines for ethical care of experimental animals of the European Union (2010/63/EU).

Electrophysiological Procedures and Data Analysis

Adult mouse ventricular cardiomyocytes were isolated as described (Delgado et al., 2015). Single rod-shaped, Ca^{2+}-tolerant myocytes were treated with calcitriol or vehicle for 15–30 min and used for electrophysiological recordings within 4 h of isolation.

The electrophysiological protocols used to record APs and K^+ currents in this study were the same as those previously described (Trépanier-Boulay et al., 2001; Brouillette et al., 2004; Gómez-Hurtado et al., 2017). Briefly, ventricular myocytes were placed in a chamber mounted on the stage of an inverted microscope and allowed to adhere for 5 min before being superfused with Tyrode's solution. Whole-cell voltage-clamp and current clamp recordings were obtained in the ruptured patch configuration using an Axopatch 200B patch clamp amplifier (Molecular Devices, Sunnyvale, CA, United States). The patch pipette resistance was 1.0–2 MΩ and the pipette was filled with a solution containing (in mM): 135 KCl, 4 $MgCl_2$, 5 EGTA, 10 HEPES, 10 glucose, 5 Na_2ATP, and 5 disodium creatine phosphate; the pH was adjusted to 7.2 with KOH. Whole-cell voltage clamp experiments were performed at room temperature (24–26°C), whereas whole-cell current clamp experiments (AP recordings) were carried out at 36–37°C.

The external solution for K^+ current recordings contained (in mM): 135 NaCl, 10 glucose, 10 HEPES, 1 $MgCl_2$, 1 $CaCl_2$, 5.4 KCl, and 2 $CoCl_2$; the pH was adjusted to 7.4 with NaOH. The external solution for AP recordings contained (in mM): 140 NaCl, 10 glucose, 10 HEPES, 1.1 $MgCl_2$, 1.8 $CaCl_2$, and 4 KCl; the pH was adjusted to 7.2 with KOH.

Current density was calculated from the current amplitude normalized to the membrane capacitance. Membrane capacitance (C_m) was elicited by applying ±10 mV voltage steps from −60 mV and C_m was calculated according to the following equation:

$$C_m = \tau_c I_0 / \Delta V_m [1 - (I_\infty / I_0)]$$

where τ_c is the time constant of the membrane capacitance, I_0 the maximum capacitance current value, ΔV_m the amplitude of the voltage step, and $I\infty$ the amplitude of the steady-state current.

In some experiments the perforated patch-clamp technique was used to record the time course of the effects of calcitriol on total K^+ currents. Perforated-patch recordings were started 5–25 min after a giga-seal was obtained. Just before use, the tip of the pipette was filled with antibiotic-free intracellular solution and the remainder of the pipette was backfilled with pipette solution containing 250 μg/mL amphotericin B. Depolarizing pulses from a holding potential of −60 to −40 mV were used to monitor the access resistance. Recordings of I_{total} were initiated when the access resistance was stabilized at 6–13 MΩ. I_{total} was elicited by depolarizing pulses to +50 mV from a holding potential of −80 mV every 10 s. The extracellular solution for I_{total} recordings for perforated-patch experiments was the same that we used for the whole-cell experiments. The intracellular solution used to elicit recordings in the perforated-patch configuration contained (in mM): 110 potassium aspartate, 20 KCl, 1 EGTA, 1 $CaCl_2$, 5 HEPES, 1 $MgCl_2$, 250 μg/mL amphotericin B; pH adjusted to 7.2 with KOH.

Western Blotting

Cardiomyocytes were homogenized in a buffer containing 320 mM sucrose, 50 mM Tris and 0.2% nonidet P-40, supplemented with a phosphatase, trypsin and protease inhibitor cocktail (Sigma-Aldrich, Madrid, Spain). Lysed cells were centrifuged at 13,000 rpm for 10 min at 4°C and the supernatants were used for immunoblotting. Equal amounts of protein were separated on 10% SDS–PAGE gels and transferred to polyvinylidene difluoride membranes. The membranes were blocked with 5% non-fat milk and incubated overnight with the following primary antibodies: phospho-Akt (Thr308) and Akt (Cell Signaling Technology, Danvers, MA, United States)., blots were incubated with peroxidase-conjugated secondary antibodies and immunoreactive bands were detected using the Amersham ECL™ protein detection system (GE Healthcare, Piscataway, NJ, United States) and medical x-ray film blue (Agfa HealthCare, Morstel, Belgium). Films were scanned with a NIKON camera and quantified by ImageJ software (NIH, Bethesda, MD, United States).

Reagents

The Akt inhibitor triciribine, calcitriol and amphotericin B were purchased from Sigma-Aldrich Co. (St. Louis, MO, United States). A stock solution of calcitriol was prepared using DMSO as vehicle (<0.01% DMSO).

Statistical Analysis

Data are presented as means ± SEM. Statistical analysis was performed with GraphPad Prism 5.0 (GraphPad Software Inc., La Jolla, CA, United States). Statistical significance was evaluated using unpaired or paired Student's *t*-test when appropriate. A value of $P < 0.05$ was considered statistically significant.

RESULTS

Calcitriol Increases Outward K^+ Currents

For the experimental setup, the main K^+ currents responsible for the AP repolarization phase in the mouse were recorded in ventricular myocytes treated either with vehicle or 10 nM calcitriol for 15–30 min. In the adult mouse ventricle, outward K^+ currents involved in cardiac repolarization comprise three components that can be distinguished by their specific time and voltage dependency and also their sensitivity to pharmacological agents. **Figure 1** illustrates the protocol used to identify the three components: the fast transient outward current (I_{tof}), the ultrarapid delayed rectifier K^+ current (I_{kur}) and the non-inactivating steady-state outward current (I_{ss}). As a first step the total K^+ currents were recorded by applying 300 ms depolarizing steps from −50 to +50 mV from a holding potential of −80 mV (**Figure 1A**). Then, I_{tof} was inactivated by applying a short prepulse (100 ms step at −30 mV) from a holding potential of −80 mV, followed by depolarizing steps from −50 to +50 mV. I_{tof} was then calculated by substracting the current recording with (**Figure 1A**) and without (**Figure 1B**) the inactivating prepulse. The current that remains after I_{tof} was inactivated, is composed of I_{ss} and I_{Kur}. To separate both currents, a low concentration of 4-aminopyridine (4-AP, 250 μM), which selectively blocks I_{kur}, was applied to cells that were prepulsed to inactivate I_{tof}. The current remaining after this protocol is I_{ss} (**Figure 1C**), and I_{kur} can then be obtained by subtracting the current in the absence (**Figure 1B**) and in the presence (**Figure 1C**) of 4-AP. **Figure 2A** shows representatives recordings of total K^+ currents obtained in 1 myocyte treated with vehicle and in 1 myocyte treated with 10 nM calcitriol. **Figure 2B** shows mean current-voltage (IV) curves for I_{total} density. Myocytes treated with calcitriol showed higher values of I_{total} density than those treated with vehicle (at +50 mV, vehicle 38.2 ± 2.2 pA/pF, $n = 27$; calcitriol 50.5 ± 3.1 pA/pF, $n = 30$; $P < 0.01$). In another group of experiments we tested the effect of calcitriol on total K^+ currents by analyzing the time dependence of the effect in continuous recordings. For that, we used the perforated patch-clamp technique which preserves the cell from loss of some cytosolic second messengers due to intracellular dialysis that occurs during prolonged whole-cell recordings. **Figure 2C** (upper panel) shows representative traces of I_{total} corresponding to points a, b, and c on the graph below (lower panel). Peak I_{total} was elicited by depolarizing pulses from a holding potential of −80 to +50 mV every 10 s over 19 min. Application of calcitriol induced a rapid increase in I_{total}, which reached a maximum effect at 9–10 min; then, the cardiomyocyte was perfused with calcitriol-free solution, which led to a progressive decrease in I_{total} toward control values after ∼10 min of washout. Similar results were obtained in three other cardiomyocytes.

Figure 3A (left panel) shows representative recordings of I_{tof} obtained in 1 myocyte treated with vehicle and in 1 myocyte treated with 10 nM calcitriol a, and **Figure 3A** (right panel) shows (IV) curves for I_{tof} density. Myocytes treated with calcitriol showed higher values of I_{tof} density than those treated with vehicle (at +50 mV, vehicle: 10.6. ± 0.9 pA/pF, $n = 23$; calcitriol: 15.9 ± 1.4 pA/pF, $n = 28$; $P < 0.01$). **Figure 3B**

(left panel) illustrates representative recordings of I_{kur} obtained in 1 myocyte treated with vehicle and in 1 myocyte treated with 10 nM calcitriol l), **Figure 3B** (right panel) shows mean IV curves for I_{kur} density). Myocytes treated with calcitriol showed higher values of I_{kur} density than those treated with vehicle (at +50 mV, vehicle: 13.2 ± 1.2 pA/pF, n = 25; calcitriol: 19.4 ± 1.8 pA/pF, n = 24; $P < 0.01$). Representative recordings of I_{ss} obtained in 1 myocyte treated with vehicle and in 1 myocyte treated with 10 nM calcitriol are shown in **Figure 3C** left panel, and mean IV curves for I_{ss} density are shown in **Figure 3C** right panel. I_{ss} values in myocytes treated with vehicle (at +50 mV, 12.4 ± 0.8 pA/pF, n = 12) were similar to those of myocytes treated with calcitriol (at +50 mV, 12.8 ± 0.5 pA/pF, n = 26).

Calcitriol Treatment Does Not Modify Action Potentials Duration

Since an increase in outward current can modulate repolarization, we carried out current clamp experiments to measure AP duration (APD) in myocytes treated with vehicle or calcitriol. Representative traces of APs recorded in 1 ventricular myocyte treated with vehicle (left) and in 1 myocyte treated with calcitriol (right) are shown in **Figure 4A**. Mean values of APD measured at 20, 50, and 90% of repolarization obtained in ventricular myocytes treated with vehicle or calcitriol are illustrated in **Figure 4B**. Values of APD were similar in both groups: APD20, vehicle 1.2 ± 0.6 ms vs. calcitriol 1.3 ± 0.1 ms; APD50, vehicle 3.4 ± 0.3 ms vs. calcitriol 2.9 ± 0.2 ms; APD90, vehicle 25.2 ± 3.5 ms vs. calcitriol 23.5 ± 2.5 ms (n = 10 cells treated with vehicle or calcitriol). In addition, no differences were observed in resting potential (RP) or AP amplitude in myocytes treated with vehicle or with calcitriol (−78.3 ± 1.9 mV vs. −77.4 ± 1.4 mV for RP and 117.7 ± 3.7 mV vs. 120.7 ± 3.6 mV for AP amplitude, vehicle vs. calcitriol-treated cells, respectively).

Vitamin D Receptor Is Involved in the Effect of Calcitriol on Outward K+ Currents

To examine the participation of VDR in the effect of calcitriol on I_{tof} and I_{kur}, ventricular myocytes were isolated from VDR-KO mice and treated with vehicle or 10 nM calcitriol for 15–30 min. Representative recordings of I_{tof}, obtained in 1 VDR-KO myocyte treated with vehicle or 10 nM calcitriol are shown in **Figure 5A** left panel, and mean IV curves for I_{tof} density are shown in **Figure 5A** right panel. In VDR-deficient myocytes, calcitriol was unable to increase I_{tof} density when compared with vehicle (at +50 mV, vehicle: 13.1 ± 1.8 pA/pF, n = 10; calcitriol: 12.5 ± 2.2 pA/pF, n = 6). Representative recordings of I_{kur}, obtained in 1 VDR-KO myocyte treated with vehicle and in 1 VDR-KO myocyte treated with 10 nM calcitriol are shown in **Figure 5B** (left panel), and mean IV curves for I_{kur} density are shown in **Figure 5B** right panel. In the absence of VDR, the mean I_{kur} density was similar between myocytes treated

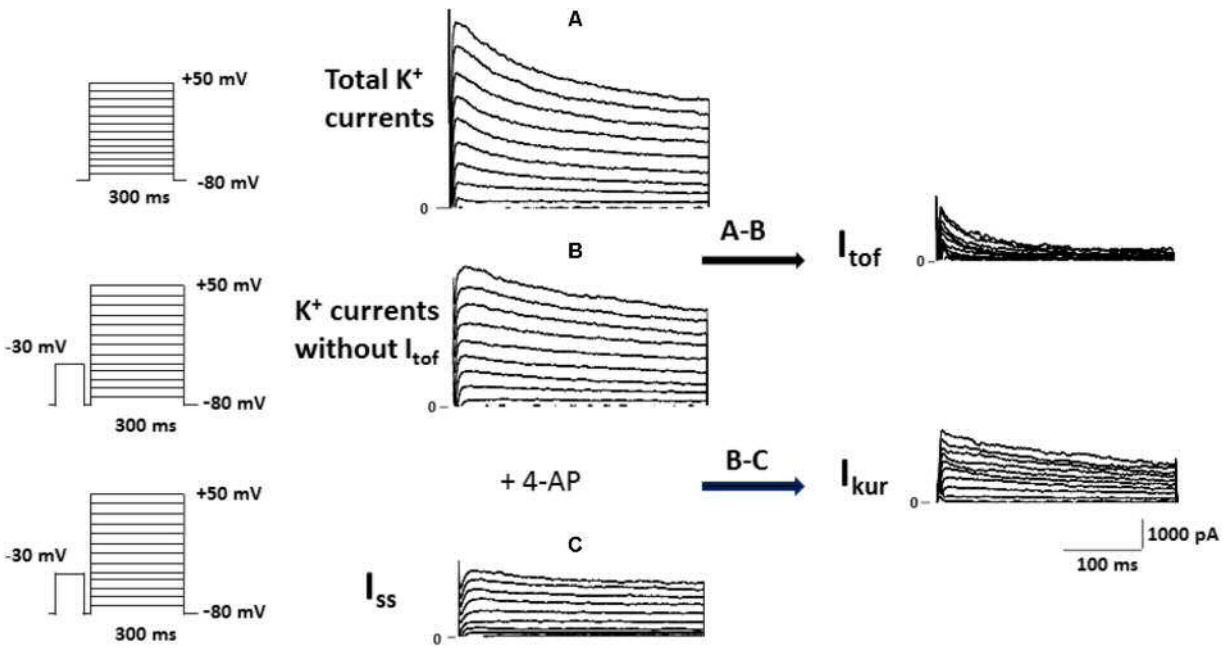

FIGURE 1 | Protocol used to isolate the fast transient outward K^+ current (I_{tof}), the ultrarapid delayed rectifier K^+ current (I_{kur}) and the non-inactivating steady-state outward current (I_{ss}) in mouse ventricular cardiomyocytes. **(A)** Superimposed current records of total K^+ currents activated by voltage protocol shown on the left. **(B)** Family of K^+ currents obtained from the same cell as in **(A)** (C_m = 212 pF), but voltage-clamp steps were each preceded by an inactivating pulse at −30 mV, shown in the left panel. I_{tof} was then calculated by substracting the current recording with **(A)** and without **(B)** the inactivating prepulse. **(C)** Superimposed current records of K^+ currents obtained after the same cell as those in **(B)** (C_m = 212 pF) was perfused with 4-AP, which selectively blocks I_{Kur}. The current remaining after this protocol is I_{ss}, and I_{kur} was then obtained by subtracting the current in the absence in the presence of 4-AP.

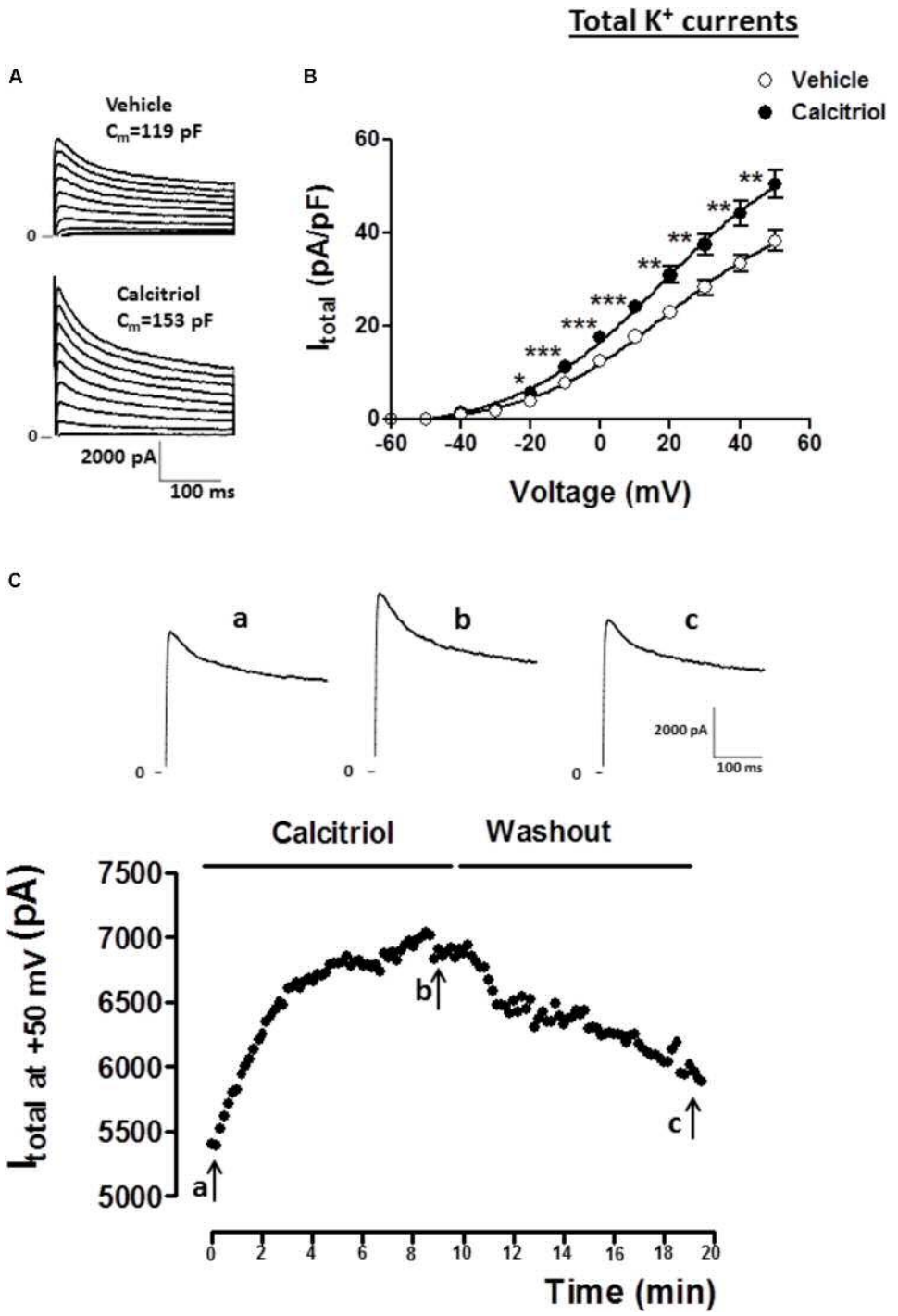

FIGURE 2 | Calcitriol increases total K^+ currents in ventricular myocytes. **(A)** Superimposed current records of total K^+ current (I_{total}) for 1 myocyte treated with vehicle and 1 myocyte treated with 10 nM calcitriol. **(B)** Current-voltage curves for I_{total} density obtained in myocytes treated with vehicle or calcitriol. **(C)** Time course of the effect of calcitriol on I_{total} by perforated patch-clamp recordings. The black points in the figure are peak outward currents recorded at +50 mV every 10 s. Horizontal line indicates exposure to calcitriol 10 nM and washout. Upper panel shows I_{total} traces at +50 mV corresponding to time 0 min **(a)**, 9 min after calcitriol perfusion **(b),** and ∼10 min after washout **(c)**. Data are expressed as means ± SEM. C_m = membrane capacitance in pF. ***$P < 0.001$; **$P < 0.01$; *$P < 0.05$.

with vehicle or calcitriol (at +50 mV, vehicle: 9.9 ± 1.0 pA/pF, n = 6; calcitriol: 11.2 ± 1.4 pA/pF, n = 9). Representative recordings of I_{ss}, obtained in 1 VDR-KO myocyte treated with vehicle and in 1 VDR-KO myocyte treated with 10 nM calcitriol are shown in **Figure 5C** (left panel), and mean IV curves for I_{ss} density in VDR-KO myocytes treated with vehicle or calcitriol are

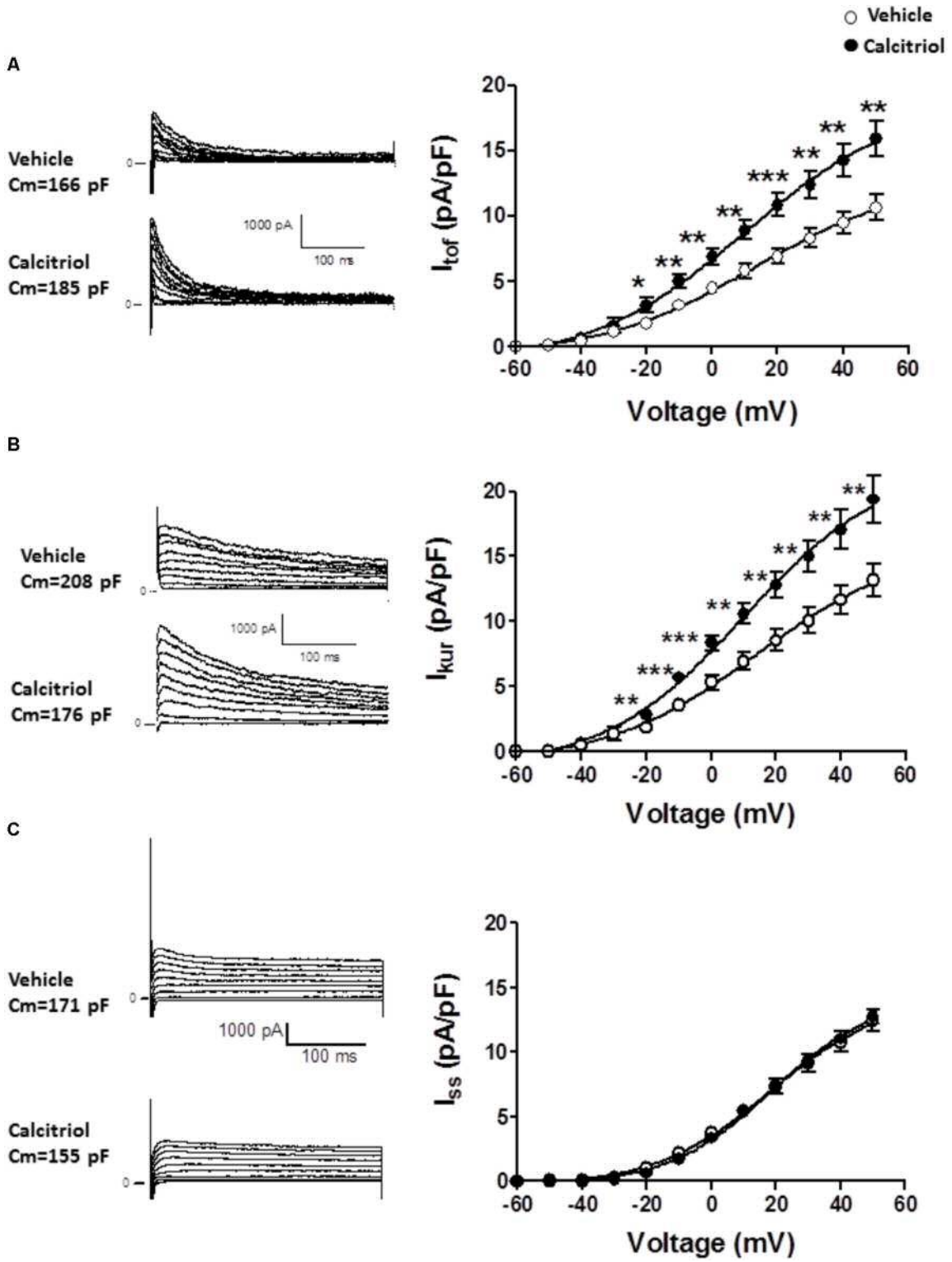

FIGURE 3 | The fast transient outward K^+ current (I_{tof}) and the ultrarapid delayed rectifier K^+ current (I_{kur}) are significantly increased in calcitriol-treated myocytes. **(A)** *Left panel*: representative I_{tof} traces for 1 myocyte treated with vehicle and 1 myocyte treated with 10 nM calcitriol. *Right panel*: I/V curves for I_{tof} density obtained in myocytes treated with vehicle or with 10 nM calcitriol. **(B)** *Left panel*: representative I_{kur} traces for 1 myocyte treated with vehicle and 1 myocyte treated with calcitriol. *Right panel*: I/V curves for I_{kur} density obtained in myocytes treated with vehicle or calcitriol. **(C)** *Left panel*: representative I_{ss} traces for 1 myocyte treated with vehicle and 1 myocyte treated with calcitriol. Data are expressed as means ± SEM. C_m = membrane capacitance in pF. ***$P < 0.001$; **$P < 0.01$; *$P < 0.05$.

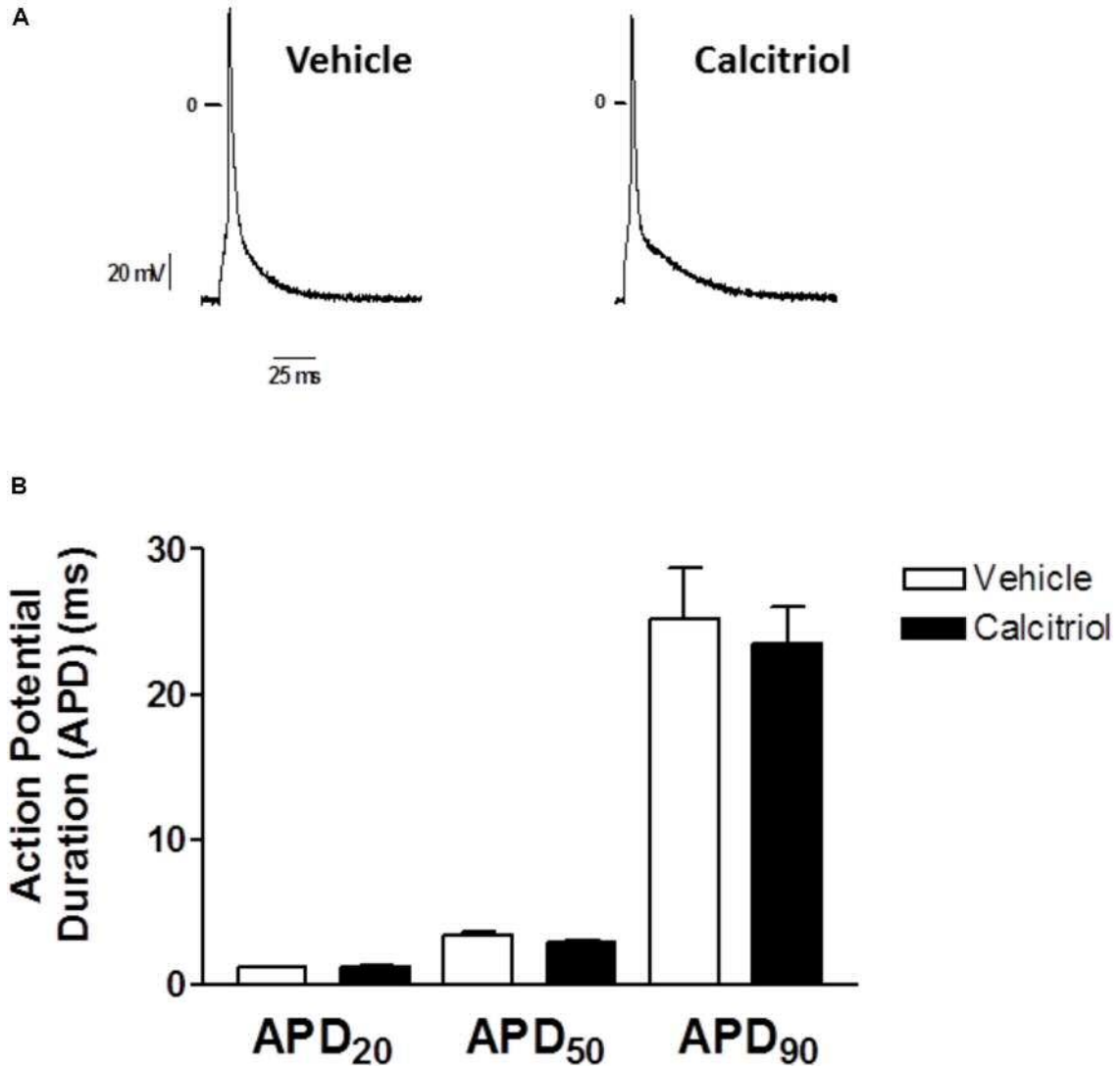

FIGURE 4 | Effects of calcitriol on Action Potentials Duration **(A)** Representative traces of action potentials recorded in 1 myocyte treated with vehicle and in 1 myocyte treated with 10 nM calcitriol. **(B)** Bar graph showing mean action potential duration (APD) values measured at 20, 50, and 90% of repolarization (APD20, APD50, and APD90, respectively). Data are expressed as means ± SEM.

shown in **Figure 5C** right panel. Results showed that calcitriol had no effect on I_{ss} density in VDR-KO myocytes (at +50 mV, vehicle: 8.7 ± 0.6 pA/pF, n = 13; calcitriol: 8.8 ± 0.6 pA/pF, n = 10).

Akt Mediates the Stimulatory Effect of Calcitriol on I_{tof} and I_{kur}

It has been postulated that the activation of the PI3K pathway can modulate cardiac K^+ channels (Yang et al., 2012; Gomez-Hurtado et al., 2014). To explore the implication of PI3K signaling in the calcitriol-induced increase of I_{tof} and I_{kur} densities, we questioned whether calcitriol activates Akt, a known target of PI3K, in ventricular myocytes (Shioi et al., 2002; McMullen et al., 2003). We observed a significant activation of Akt (measured as phosphorylation) after 15 min of calcitriol treatment (**Figures 6A,B**). We therefore measured I_{tof}, I_{kur}, and I_{ss} in myocytes pretreated with 1 μM of the Akt inhibitor triciribine. Representative traces obtained in myocytes pretreated with triciribine and then treated with vehicle or calcitriol are shown in **Figures 7A–C**, respectively (left panels), and mean IV curves for I_{tof}, I_{kur} and I_{ss} densities in both situations are shown in the corresponding right panels. The results showed that treatment with triciribine prevented the stimulatory effect of calcitriol on I_{tof} and I_{Kur}.

DISCUSSION

Cardiac APs are the consequence of the coordinated functioning of inward and outward current flowing through specialized

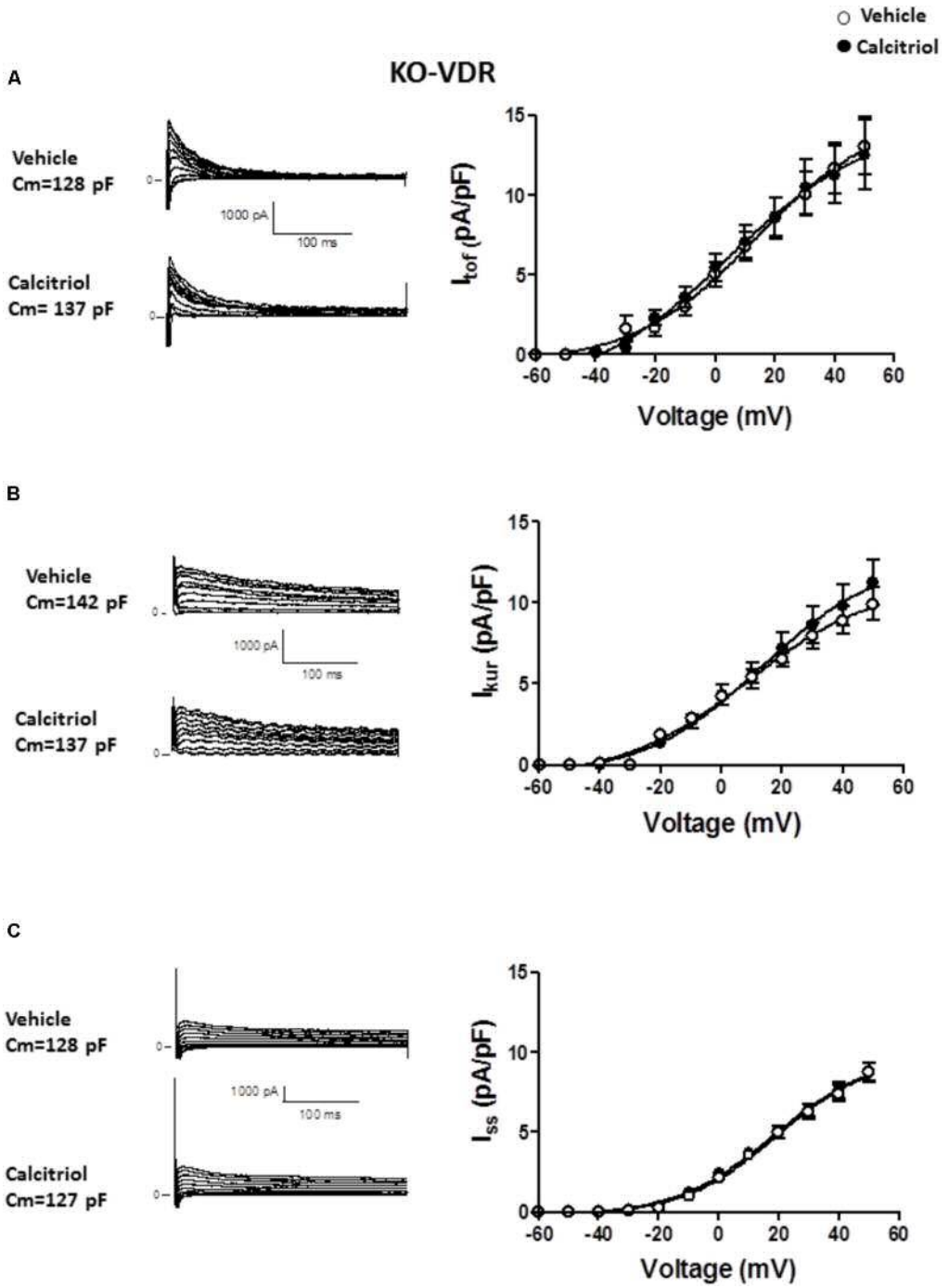

FIGURE 5 | Effect of calcitriol on I_{tof} and I_{kur} involves binding to the vitamin D receptor. **(A)** *Left panel*: representative traces of I_{tof} obtained in 1 VDR-KO myocyte treated with vehicle and in 1 VDR-KO myocyte treated with 10 nM calcitriol. *Right panel*: I/V curves for I_{tof} density obtained in VDR-KO myocytes treated with vehicle or calcitriol. **(B)** *Left panel*: representative traces of I_{kur} obtained in 1 VDR-KO myocyte treated with vehicle and in 1 VDR-KO myocyte treated with 10 nM calcitriol. *Right panel*: I/V curves for I_{kur} density obtained in VDR-KO myocytes treated with vehicle or calcitriol. **(C)** *Left panel*: representative traces of I_{ss} obtained in 1 VDR-KO myocyte treated with vehicle and in 1 VDR-KO myocyte treated with 10 nM calcitriol. *Right panel*: I/V curves for I_{ss} density obtained in VDR-KO myocytes treated with vehicle or calcitriol. Data are expressed as means ± SEM. C_m = membrane capacitance in pF.

proteins (ionic channels) that open and close in a voltage- and time-dependent manner allowing rhythmic and effective cardiac contractions (Gaborit et al., 2007). It is well known that K^+ current density is reduced during heart remodeling under various pathological conditions including left ventricular hypetrophy and HF. This process is associated with prolonged QT interval,

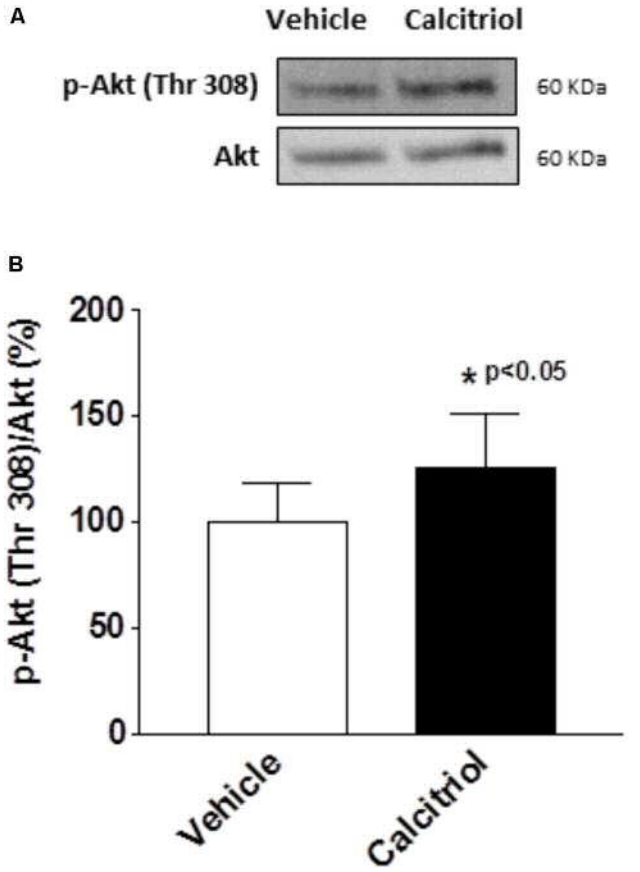

FIGURE 6 | Calcitriol activates the Akt pathway in ventricular myocytes. Ventricular myocytes were exposed to vehicle or calcitriol 10 nM for 15 min. **(A)** Representative western blot and **(B)** average ratio of protein levels expressed as the percentage of phospho (P)-Akt normalized to total Akt. Data are expressed as mean ± SEM. $^*P < 0.05$.

increased risk of malignant arrhythmias and sudden cardiac death (Ravens and Cerbai, 2008). Here, we tested the hypothesis that calcitriol might have a cardioprotective effect by increasing K^+ currents, thereby circumventing inappropriate prolongation" of the APD during pathology. In mice, the repolarization phase of the AP is determined principally by the outward currents I_{tof} and I_{kur}, which account for the remarkably abbreviated APs and the absence of a clear plateau phase in this species. We found that calcitriol significantly increased I_{tof} and I_{kur} densities. In apparent contrast, we found that the APD was similar in myocytes treated or not with calcitriol. The lack of the effect of increased K^+ currents on the APD in calcitriol-treated myocytes indicates that calcitriol might affect other ionic currents that influence the APD. In this sense, we previously demonstrated that calcitriol can increase L-type calcium current (I_{CaL}) density in ventricular myocytes (Tamayo et al., 2017). The increase of I_{CaL} might counterbalance the effect of increased outward K^+ currents in calcitriol-treated myocytes, preserving the APD. Calcitriol can induce genomic (transcription-dependent) and non-genomic (transcription-independent) actions. Indeed, there is a general agreement in the idea that calcitriol effects observed within minutes (such as those described in the present study) involve only non-genomic effects mediated by extra-nuclear mechanisms (Mizwicki and Norman, 2009). Most calcitriol actions are mediated by VDR. Classic nuclear VDR is required for genomic effects, whereas non-genomic actions are thought to be mediated by a fraction of VDR located in the cytosol or at the plasma membrane (Norman et al., 2001a,b). In this regards, *in silico* studies have been useful to determine exactly how calcitriol binds to VDR to regulate both genomic and non-genomic responses. An alternative ligand-binding pocket has been identified in VDR that specifically mediates non-genomic actions and that partially overlaps the genomic pocket described in the experimentally determined x-ray structure (Mizwicki et al., 2004). In the present study, we used VDR-KO mice to determine whether the effect of calcitriol on K^+ currents in cardiomyocytes involves VDR. Our results clearly show that the absence of VDR abolished all changes in K^+ currents induced by the acute administration of calcitriol, demonstrating that these effects are VDR-dependent. Consistent with this, we have previously described that calcitriol exerts VDR-dependent non-genomic effects on Ca^{2+} current and PKA signaling in cardiomyocytes (Tamayo et al., 2017), which is in line with the findings by Zanello and Norman (2006) showing that a functional VDR is required for the rapid increase in Cl- current and for the shift in the peak activation of I_{CaL} current induced by calcitriol in osteoblasts. As VDR-KO mice do not express VDR, this model does not allow us to discriminate precisely which VDR location mediates these observed effects. We are, however, inclined to favor a non-genomic action mediated by membrane VDR due to the short time required (15–30 min) and the fact that VDR has been reported to be expressed in the tubular system of ventricular myocytes (Tishkoff et al., 2008), a region where voltage-gated calcium and potassium channels are predominantly localized (Takeuchi et al., 2000; Brette and Orchard, 2003). On the other hand, protein disulfide isomerase family A member 3 (PDIA3) has been proposed as a membrane receptor for calcitriol that mediates some of its non-genomic effects in chondrocytes, osteoblasts and other cell types (Boyan et al., 2003; Doroudi et al., 2014a,b). Intriguingly, both PDIA3 and VDR are located in caveolae in many tissues and cell types, and an interaction between them has been observed, suggesting that VDR and PDIA3 might both be required for some non-genomic actions of calcitriol (Sequeira et al., 2012; Chen et al., 2013). As the effects of calcitriol on K^+ current in cardiomyocytes are completely abolished in VDR-KO cells we would argue that PDIA3 is not implicated in the described effect, although clearly experiments with PDIA3-KO cells would be necessary to completely discard the possibility that both VDR and PDIA3 are involved.

Several reports have shown that calcitriol binding to plasma membrane VDR induces rapid non-transcriptional responses through the activation of different signaling pathways including PI3K/Akt (Buitrago et al., 2012; Salles et al., 2013). This pathway is widely expressed in eukaryotes and is known to play key roles in growth, differentiation, proliferation, and survival (Cantley, 2002). In the heart,

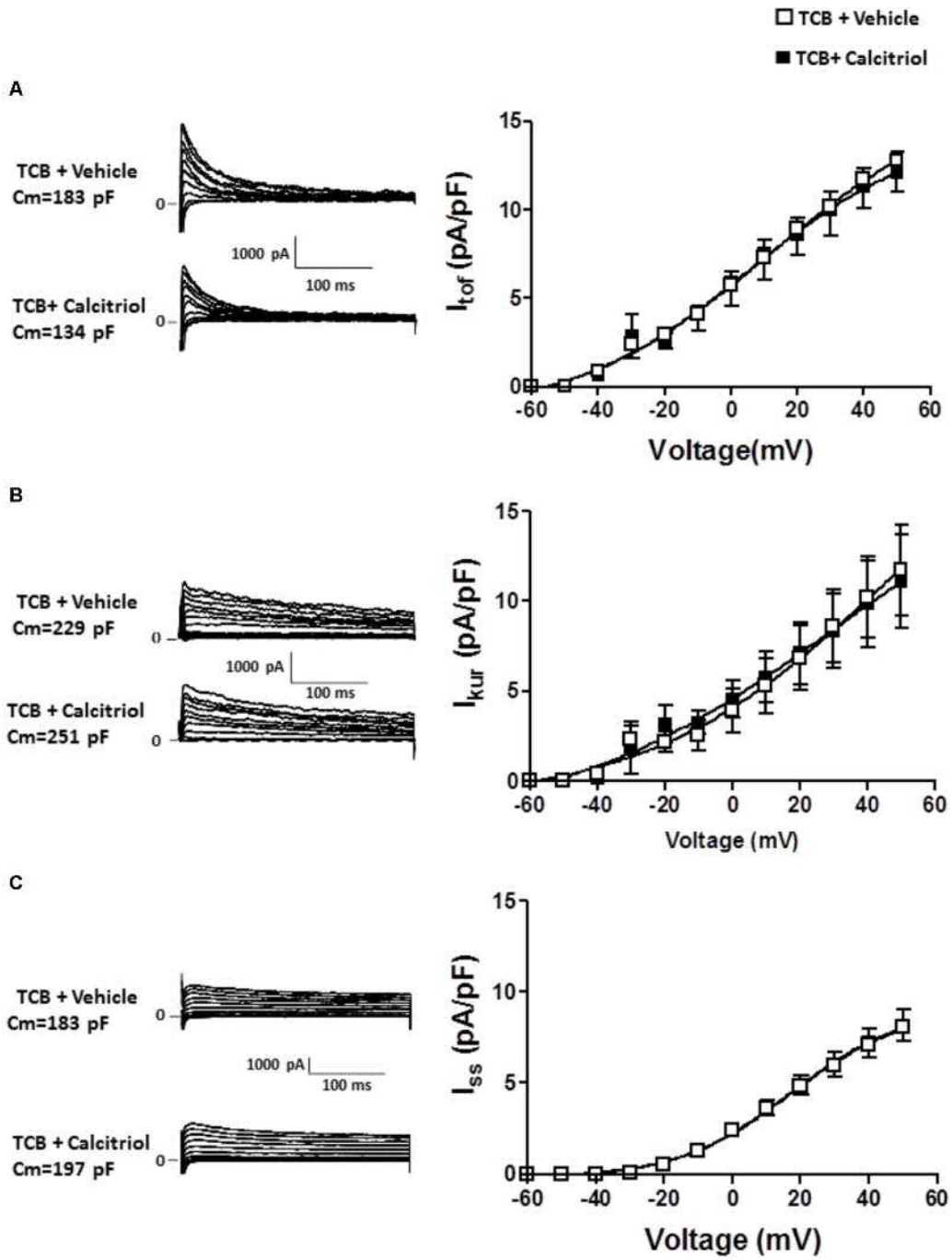

FIGURE 7 | Inhibition of Akt signaling prevents the increase in I_{tof} and I_{kur} densities induced by calcitriol. **(A)** *Left panel*: I_{tof} traces obtained in 1 myocyte treated with 1 μM triciribine and in 1 myocyte treated with 1 μM triciribine plus 10 nM calcitriol. *Right panel*: I/V curves for I_{tof} density obtained in myocytes treated with 1 μM triciribine or with triciribine plus 10 nM calcitriol. **(B)** *Left panel*: I_{kur} traces obtained in one myocyte treated with 1 μM triciribine and in 1 myocyte treated with 1 μM triciribine plus 10 nM calcitriol. *Right panel*: I/V curves for I_{kur} density obtained in myocytes treated with 1 μM triciribine or with triciribine plus 10 nM calcitriol. **(C)** *Left panel*: I_{ss} traces obtained in 1 myocyte treated with 1 μM triciribine and in 1 myocyte treated with 1 μM triciribine plus 10 nM calcitriol. *Right panel*: I/V curves for I_{ss} density obtained in myocytes treated with 1 μM triciribine or with triciribine plus 10 nM calcitriol. Data are expressed as means ± SEM. C_m, membrane capacitance; TCB, triciribine.

PI3K/Akt activation has been related to both physiological cardiac enlargement and protection (McMullen et al., 2003; Weeks et al., 2012). Moreover, it is believed that the PI3K/Akt pathway might regulate cardiac ion channels and arrhythmogenesis (Ballou et al., 2015). Our results show that calcitriol activates Akt in adult ventricular myocytes, and

its pharmacological inhibition prevents the calcitriol-induced increase of I_{tof} and I_{kur} densities.

In sum, we demonstrate that calcitriol binding to VDR increases the density of the two main K^+ currents responsible for the rapid repolarization of the AP in the mouse, I_{tof} and I_{Kur}. Our study also supports a role of Akt signaling in this stimulatory effect.

AUTHOR CONTRIBUTIONS

MT performed most of the experiments and analyzed the data. LM-N isolated ventricular myocytes and performed most of the western blotting experiments. MP took part in the critical discussion and editing of the manuscript. ML provided VDR-KO mice. AV-B and NG-H helped with western blotting. ML and NG-H took part in the critical discussion and editing of the manuscript. MF-V designed the experiments, reviewed the data, and wrote the manuscript. CD performed some electrophysiological experiments, conceived the hypothesis, supervised the project, reviewed the data, and wrote the manuscript.

FUNDING

This work was supported by grants SAF2014-57190R, SAF2017-84777R, and SAF2016-76377R from the Spanish Ministerio de Industria, Economia y Competitividad and PI14/01078 and PI17/01344 from ISCIII, Fondos FEDER and CIBER-CV and CIBERONC, networks funded by ISCIII.

ACKNOWLEDGMENTS

We thank Drs. M.B. Demay and A. Muñoz for providing VDR-KO mice. We are grateful to María Gracia González-Bueno for her technical assistance and Dr. Kenneth McCreath for English editing.

REFERENCES

Ballou, L. M., Lin, R. Z., and Cohen, I. S. (2015). Control of cardiac repolarization by phosphoinositide 3-kinase signaling to ion channels. *Circ. Res.* 116, 127–137. doi: 10.1161/CIRCRESAHA.116.303975

Boyan, B. D., Sylvia, V. L., McKinney, N., and Schwartz, Z. (2003). Membrane actions of vitamin D metabolites 1alpha,25(OH)2D3 and 24R,25(OH)2D3 are retained in growth plate cartilage cells from vitamin D receptor knockout mice. *J. Cell. Biochem.* 90, 1207–1223. doi: 10.1002/jcb.10716

Brette, F., and Orchard, C. (2003). T-tubule function in mammalian cardiac myocytes. *Circ. Res.* 92, 1182–1192. doi: 10.1161/01.RES.0000074908.17214.FD

Brouillette, J., Clark, R. B., Giles, W. R., and Fiset, C. (2004). Functional properties of K+ currents in adult mouse ventricular myocytes. *J. Physiol.* 559, 777–798. doi: 10.1113/jphysiol.2004.063446

Buitrago, C. G., Arango, N. S., and Boland, R. L. (2012). 1α,25(OH)2D3-dependent modulation of Akt in proliferating and differentiating C2C12 skeletal muscle cells. *J. Cell. Biochem.* 113, 1170–1181. doi: 10.1002/jcb.23444

Cantley, L. C. (2002). The phosphoinositide 3-kinase pathway. *Science* 296, 1655–1657. doi: 10.1126/science.296.5573.1655

Chen, J., Doroudi, M., Cheung, J., Grozier, A. L., Schwartz, Z., and Boyan, B. D. (2013). Plasma membrane Pdia3 and VDR interact to elicit rapid responses to 1α,25(OH)(2)D(3). *Cell. Signal.* 25, 2362–2373. doi: 10.1016/j.cellsig.2013.07.020

Delgado, C., Ruiz-Hurtado, G., Gomez-Hurtado, N., Gonzalez-Ramos, S., Rueda, A., Benito, G., et al. (2015). NOD1, a new player in cardiac function and calcium handling. *Cardiovasc. Res.* 106, 375–386. doi: 10.1093/cvr/cvv118

Doroudi, M., Boyan, B. D., and Schwartz, Z. (2014a). Rapid 1α,25$(OH)_2D_3$ membrane-mediated activation of Ca^{2+}/calmodulin-dependent protein kinase II in growth plate chondrocytes requires Pdia3. PLAA and caveolae. *Connect. Tissue Res.* 55(Suppl. 1), 125–128.

Doroudi, M., Chen, J., Boyan, B. D., and Schwartz, Z. (2014b). New insights on membrane mediated effects of 1α,25-dihydroxy vitamin D3 signaling in the musculoskeletal system. *Steroids* 81, 81–87. doi: 10.1016/j.steroids.2013.10.019

Gaborit, N., Le Bouter, S., Szuts, V., Varro, A., Escande, D., Nattel, S., et al. (2007). Regional and tissue specific transcript signatures of ion channel genes in the non-diseased human heart. *J. Physiol.* 582, 675–693. doi: 10.1113/jphysiol.2006.126714

Gómez-Hurtado, N., Domínguez-Rodríguez, A., Mateo, P., Fernández-Velasco, M., Val-Blasco, A., Aizpún, R., et al. (2017). Beneficial effects of leptin treatment in a setting of cardiac dysfunction induced by transverse aortic constriction in mouse. *J. Physiol.* 595, 4227–4243. doi: 10.1113/JP274030

Gomez-Hurtado, N., Fernandez-Velasco, M., Fernandez-Alfonso, M., Bosca, L., and Delgado, C. (2014). Prolonged leptin treatment increases transient outward K+ current via upregulation of Kv4.2 and Kv4.3 channel subunits in adult rat ventricular myocytes. *Pflugers Arch.* 466, 903–914. doi: 10.1007/s00424-013-1348-3

Gotsman, I., Shauer, A., Zwas, D. R., Hellman, Y., Keren, A., Lotan, C., et al. (2012). Vitamin D deficiency is a predictor of reduced survival in patients with heart failure; vitamin D supplementation improves outcome. *Eur. J. Heart Fail.* 14, 357–366. doi: 10.1093/eurjhf/hfr175

Hartupee, J., and Mann, D. L. (2017). Neurohormonal activation in heart failure with reduced ejection fraction. *Nat. Rev. Cardiol.* 14, 30–38. doi: 10.1038/nrcardio.2016.163

Heusch, G., Libby, P., Gersh, B., Yellon, D., Böhm, M., Lopaschuk, G., et al. (2014). Cardiovascular remodelling in coronary artery disease and heart failure. *Lancet* 383, 1933–1943. doi: 10.1016/S0140-6736(14)60107-0

Holick, M. F. (2007). Vitamin D deficiency. *N. Engl. J. Med.* 357, 266–281. doi: 10.1056/NEJMra070553

Larriba, M. J., González-Sancho, J. M., Bonilla, F., and Muñoz, A. (2014). Interaction of vitamin D with membrane-based signaling pathways. *Front. Physiol.* 5:60. doi: 10.3389/fphys.2014.00060

Lehnart, S. E., Maier, L. S., and Hasenfuss, G. (2009). Abnormalities of calcium metabolism and myocardial contractility depression in the failing heart. *Heart Fail. Rev.* 14, 213–224. doi: 10.1007/s10741-009-9146-x

Li, Y. C., Pirro, A. E., Amling, M., Delling, G., Baron, R., Bronson, R., et al. (1997). Targeted ablation of the vitamin D receptor: an animal model of vitamin D-dependent rickets type II with alopecia. *Proc. Natl. Acad. Sci. U.S.A.* 94, 9831–9835. doi: 10.1073/pnas.94.18.9831

Liu, L. C., Voors, A. A., van Veldhuisen, D. J., van der Veer, E., Belonje, A. M., Szymanski, M. K., et al. (2011). Vitamin D status and outcomes in heart failure patients. *Eur. J. Heart Fail.* 13, 619–625. doi: 10.1093/eurjhf/hfr032

Ma, Y., Yu, W. D., Kong, R. X., Trump, D. L., and Johnson, C. S. (2006). Role of nongenomic activation of phosphatidylinositol 3-kinase/Akt and mitogen-activated protein kinase/extracellular signal-regulated kinase kinase/extracellular signal-regulated kinase 1/2 pathways in 1,25D3-mediated apoptosis in squamous cell carcinoma cells. *Cancer Res.* 66, 8131–8138. doi: 10.1158/0008-5472.CAN-06-1333

McMullen, J. R., Shioi, T., Zhang, L., Tarnavski, O., Sherwood, M. C., Kang, P. M., et al. (2003). Phosphoinositide 3-kinase(p110alpha) plays a critical role for the induction of physiological, but not pathological, cardiac hypertrophy. *Proc. Natl. Acad. Sci. U.S.A.* 100, 12355–12360. doi: 10.1073/pnas.1934654100

Menegaz, D., Mizwicki, M. T., Barrientos-Duran, A., Chen, N., Henry, H. L., and Norman, A. W. (2011). Vitamin D receptor (VDR) regulation of voltage-gated

chloride channels by ligands preferring a VDR-alternative pocket (VDR-AP). *Mol. Endocrinol.* 25, 1289–1300. doi: 10.1210/me.2010-0442

Mizwicki, M. T., Keidel, D., Bula, C. M., Bishop, J. E., Zanello, L. P., Wurtz, J. M., et al. (2004). Identification of an alternative ligand-binding pocket in the nuclear vitamin D receptor and its functional importance in 1alpha,25(OH)2-vitamin D3 signaling. *Proc. Natl. Acad. Sci. U.S.A.* 101, 12876–12881. doi: 10.1073/pnas.0403606101

Mizwicki, M. T., and Norman, A. W. (2009). The vitamin D sterol-vitamin D receptor ensemble model offers unique insights into both genomic and rapid-response signaling. *Sci. Signal.* 2:re4. doi: 10.1126/scisignal.275re4

Nass, R. D., Aiba, T., Tomaselli, G. F., and Akar, F. G. (2008). Mechanisms of disease: ion channel remodeling in the failing ventricle. *Nat. Clin. Pract. Cardiovasc. Med.* 5, 196–207. doi: 10.1038/ncpcardio1130

Nattel, S., Maguy, A., Le Bouter, S., and Yeh, Y. H. (2007). Arrhythmogenic ion-channel remodeling in the heart: heart failure, myocardial infarction, and atrial fibrillation. *Physiol. Rev.* 87, 425–456. doi: 10.1152/physrev.00014.2006

Norman, A. W., Henry, H. L., Bishop, J. E., Song, X. D., Bula, C., and Okamura, W. H. (2001a). Different shapes of the steroid hormone 1alpha,25(OH)(2)-vitamin D(3) act as agonists for two different receptors in the vitamin D endocrine system to mediate genomic and rapid responses. *Steroids* 66, 147–158.

Norman, A. W., Ishizuka, S., and Okamura, W. H. (2001b). Ligands for the vitamin D endocrine system: different shapes function as agonists and antagonists for genomic and rapid response receptors or as a ligand for the plasma vitamin D binding protein. *J. Steroid Biochem. Mol. Biol.* 76, 49–59. doi: 10.1016/S0960-0760(00)00145-X

Norman, P. E., and Powell, J. T. (2014). Vitamin D and cardiovascular disease. *Circ. Res.* 114, 379–393. doi: 10.1161/CIRCRESAHA.113.301241

[illegible]s, J., Chanet, A., Giraudet, C., Patrac, V., Pierre, P., Jourdan, M., et al. (2013). 1,25(OH)2-vitamin D3 enhances the stimulating effect of leucine and insulin on protein synthesis rate through Akt/PKB and mTOR mediated pathways in murine C2C12 skeletal myotubes. *Mol. Nutr. Food Res.* 57, 2137–2146. doi: 10.1002/mnfr.201300074

Sequeira, V. B., Rybchyn, M. S., Tongkao-On, W., Gordon-Thomson, C., Malloy, P. J., Nemere, I., et al. (2012). The role of the vitamin D receptor and ERp57 in photoprotection by 1α,25-dihydroxyvitamin D3. *Mol. Endocrinol.* 26, 574–582. doi: 10.1210/me.2011-1161

Shioi, T., McMullen, J. R., Kang, P. M., Douglas, P. S., Obata, T., Franke, T. F., et al. (2002). Akt/protein kinase B promotes organ growth in transgenic mice. *Mol. Cell. Biol.* 22, 2799–2809. doi: 10.1128/MCB.22.8.2799-2809.2002

Takeuchi, S., Takagishi, Y., Yasui, K., Murata, Y., Toyama, J., and Kodama, I. (2000). Voltage-gated K(+)Channel, Kv4.2, localizes predominantly to the transverse-axial tubular system of the rat myocyte. *J. Mol. Cell. Cardiol.* 32, 1361–1369. doi: 10.1006/jmcc.2000.1172

Tamayo, M., Manzanares, E., Bas, M., Martin-Nunes, L., Val-Blasco, A., Larriba, M. J., et al. (2017). Calcitriol (1,25-dihydroxyvitamin D3) increases L-type calcium current via protein kinase A signaling and modulates calcium cycling and contractility in isolated mouse ventricular myocytes. *Heart Rhythm* 14, 432–439. doi: 10.1016/j.hrthm.2016.12.013

Tishkoff, D. X., Nibbelink, K. A., Holmberg, K. H., Dandu, L., and Simpson, R. U. (2008). Functional vitamin D receptor (VDR) in the t-tubules of cardiac myocytes: VDR knockout cardiomyocyte contractility. *Endocrinology* 149, 558–564. doi: 10.1210/en.2007-0805

Trépanier-Boulay, V., St-Michel, C., Tremblay, A., and Fiset, C. (2001). Gender-based differences in cardiac repolarization in mouse ventricle. *Circ. Res.* 89, 437–444. doi: 10.1161/hh1701.095644

Vertino, A. M., Bula, C. M., Chen, J. R., Almeida, M., Han, L., Bellido, T., et al. (2005). Nongenotropic, anti-apoptotic signaling of 1alpha,25(OH)2-vitamin D3 and analogs through the ligand binding domain of the vitamin D receptor in osteoblasts and osteocytes. Mediation by Src, phosphatidylinositol 3-, and JNK kinases. *J. Biol. Chem.* 280, 14130–14137. doi: 10.1074/jbc.M410720200

Weeks, K. L., Gao, X., Du, X. J., Boey, E. J., Matsumoto, A., Bernardo, B. C., et al. (2012). Phosphoinositide 3-kinase p110α is a master regulator of exercise-induced cardioprotection and PI3K gene therapy rescues cardiac dysfunction. *Circ. Heart Fail.* 5, 523–534. doi: 10.1161/CIRCHEARTFAILURE.112.966622

Witte, K. K., Byrom, R., Gierula, J., Paton, M. F., Jamil, H. A., Lowry, J. E., et al. (2016). Effects of Vitamin D on cardiac function in patients with chronic HF: the vindicate Study. *J. Am. Coll. Cardiol.* 67, 2593–2603. doi: 10.1016/j.jacc.2016.03.508

Yang, K. C., Jay, P. Y., McMullen, J. R., and Nerbonne, J. M. (2012). Enhanced cardiac PI3Kα signalling mitigates arrhythmogenic electrical remodelling in pathological hypertrophy and heart failure. *Cardiovasc. Res.* 93, 252–262. doi: 10.1093/cvr/cvr283

Zanatta, L., Goulart, P. B., Gonçalves, R., Pierozan, P., Winkelmann-Duarte, E. C., Woehl, V. M., et al. (2012). 1α,25-dihydroxyvitamin D(3) mechanism of action: modulation of L-type calcium channels leading to calcium uptake and intermediate filament phosphorylation in cerebral cortex of young rats. *Biochim. Biophys. Acta* 1823, 1708–1719. doi: 10.1016/j.bbamcr.2012.06.023

Zanello, L. P., and Norman, A. (2006). 1alpha,25(OH)2 vitamin D3 actions on ion channels in osteoblasts. *Steroids* 71, 291–297. doi: 10.1016/j.steroids.2005.09.012

Zhang, L., Yan, X., Zhang, Y. L., Bai, J., Hidru, T. H., Wang, Q. S., et al. (2018). Vitamin D attenuates pressure overload-induced cardiac remodeling and dysfunction in mice. *J. Steroid Biochem. Mol. Biol.* 178, 293–302. doi: 10.1016/j.jsbmb.2018.01.009 Q9

Zhang, X., and Zanello, L. P. (2008). Vitamin D receptor-dependent 1 alpha,25(OH)2 vitamin D3-induced anti-apoptotic PI3K/AKT signaling in osteoblasts. *J. Bone Miner. Res.* 23, 1238–1248. doi: 10.1359/jbmr.080326

Zhang, Y., Zhang, J., and Studzinski, G. P. (2006). AKT pathway is activated by 1, 25-dihydroxyvitamin D3 and participates in its anti-apoptotic effect and cell cycle control in differentiating HL60 cells. *Cell Cycle* 5, 447–451. doi: 10.4161/cc.5.4.2467

Conflict of Interest Statement: The authors declare that the research was conducted in the absence of any commercial or financial relationships that could be construed as a potential conflict of interest.